

# Real-time imaging with a hyperspectral fovea

David William Fletcher-Holmes and Andrew Robert Harvey<sup>1</sup>

School of Engineering and Physical Sciences, Heriot-Watt University, Riccarton, Edinburgh EH14 4AS, UK

E-mail: a.r.harvey@hw.ac.uk

Received 2 December 2004, accepted for publication 24 February 2005

Published 9 May 2005

Online at [stacks.iop.org/JOptA/7/S298](http://stacks.iop.org/JOptA/7/S298)

## Abstract

We address the two dominant dilemmas encountered in attempting to demonstrate real-time hyperspectral imaging: how to record a three-dimensional spectral data cube with a conventional two-dimensional detector array and how to most efficiently transmit the spectral data cube through the information bottleneck constituted by the detector's limited space–bandwidth product. We have demonstrated a new, biologically inspired approach in which a compact hyperspectral fovea is embedded within a conventional panchromatic periphery. Combined with an intelligent scanning system this will enable hyperspectral imaging to be applied only to small regions of interest previously identified using the panchromatic periphery, thus improving the efficiency with which hyperspectral imaging can be used to recognize objects in a scene. The hyperspectral fovea is realized using a coherent optical fibre bundle that reformats a two-dimensional input image into a linear output image that acts as the input to a one-dimensional, dispersive hyperspectral imager.

**Keywords:** hyperspectral imaging, remote sensing

(Some figures in this article are in colour only in the electronic version)

 This article features online multimedia enhancements

## 1. Introduction

Whereas for conventional imaging, panchromatic or trichromatic data are recorded for each scene pixel, hyperspectral imaging (HSI) involves the recording of many, typically hundreds, of spectral bands for each pixel. The increased information content of the recorded data has enabled improved classification and quantification of image components in fields such as remote sensing [1] and biological imaging [2]. Application of HSI has tended to be restricted to those applications where the relative stability of the scene and imager is amenable to the application of traditional spectral imaging techniques. For example, in remote sensing of the Earth from space-borne or air-borne platforms it is common to employ a time-sequential push-broom or whisk-broom scan of the footprint of a one-dimensional hyperspectral imager to enable the subsequent assembly of a two-dimensional hyperspectral

image. In laboratory-based applications, such as spectral imaging in cytology, it is convenient to assemble the spectral data cube from two-dimensional, narrow-band images recorded in time sequence. One-dimensional and two-dimensional Fourier-transform imaging spectrometers are also commonly used in both applications [3, 4]. Whichever technique is used, it is necessary to record a so-called spectral data cube and, as typified by the above example, this is conventionally achieved by either spatial or spectral multiplexing of time-sequential images onto a two-dimensional detector array.

It is also desirable to record hyperspectral, two-dimensional image data of time-varying and transient phenomena for which these time-sequential techniques cannot be used. Applications include ophthalmology [5, 6], the study of combustion dynamics [7], cellular dynamics [8] and surveillance [9]. For such applications, and for when there is relative motion between the imager and scene, the use of time-sequential HSI introduces the possibility of spatial misregistration of images and a consequent distortion of the

<sup>1</sup> Author to whom any correspondence should be addressed.  
<http://www.ece.eps.hw.ac.uk/~arharvey>.

recorded spectra [9]. Spectral distortion can be avoided by use of a snapshot HSI technique where all voxels of the spectral data cube are recorded simultaneously. To date, four techniques have been reported that record two-dimensional spectral images in a snapshot:

- (1) conventional colour imaging employing dichroic filters, either at the detector or multiplexed onto several detectors,
- (2) computed tomographic imaging spectrometry [10] in which a diffractive array generator placed in the exit pupil of a conventional imager generates multiple, spectrally smeared images on a single detector array,
- (3) image replication imaging spectrometry reported by the authors [11, 12] in which multiple narrow-band images are replicated onto a single detector array and
- (4) integral field spectroscopy (IFS) [13] in which reflective optics are used to convert a two-dimensional image into a one-dimensional image suitable for application to a one-dimensional hyperspectral imager.

The spectral resolution of all but the latter of these techniques is limited by the trading of spectral resolution against field of view so that spectral resolution is limited to, typically, a few tens of bands. This issue is directly related to the information bottleneck constituted by the space–bandwidth product of the detector array; to demonstrate two-dimensional, video-rate, hyperspectral imaging (that is, hundreds of spectral bands) with megapixel spatial resolution requires images to be recorded at the order of  $10 \text{ Gpixels s}^{-1}$ . This is about three orders of magnitude greater than the maximum pixel-rate per tap that is available with current detector arrays. Real-time processing of data at these high rates is also not currently practical. Mammalian vision systems exhibit a similar information bottleneck between the retina and the brain and this is mitigated by use of a fovea with increased spectral and spatial acuity combined with a lower acuity periphery. Regions of interest detected in the periphery are used to cue the attention of the fovea. This approach massively improves the efficiency with which important information within a scene is transmitted to and processed by the brain.

We report here a demonstration of a biologically inspired imaging system called foveal hyperspectral imaging (FHI) that employs a hyperspectral fovea with a panchromatic periphery. Image reformatting is central to both FHI and IFS; however, whereas the latter is appropriate for astronomy where relaxed budgetary and logistical constraints enable massive beam steering systems with multiple high-cost detector arrays, FHI results in a low-cost and compact handheld hyperspectral imager suitable for applications such as surveillance and biological imaging. In these applications the panchromatic peripheral image may be used for situational awareness and to screen for potential threats or abnormalities that stimulate human or automated scanning of the hyperspectral fovea to that region of interest for recognition or detailed characterization.

In section 2 we describe the instrumentation issues of the proof-of-principle demonstration of the FHI and its calibration. Classification and presentation of images is described in section 3 and conclusions in section 4.

## 2. Implementation of FHI

### 2.1. Principle of operation of FHI

The output image of FHI consists of a small, square hyperspectral image, (the hyperspectral fovea) co-registered and embedded centrally within a larger panchromatic peripheral image. Processing of the spectral data recorded within the fovea is used to construct a false-colour representation of the foveal image. The FHI concept is depicted in figure 1. The scene is relayed to the foveal and peripheral imaging systems via an intermediate image formed by the input lens, L1. A small mirror, M, and lens L2 relay the central, foveal region onto a fibre optic reformatter whilst the light not intercepted by M is relayed by lens L3 to a panchromatic charge-coupled device (CCD) array. The fibre optic reformatter (FOR) is a custom-built, coherent fibre bundle that maps a square array of fibres at its input face into a linear array at its output face. The FOR is mounted onto a commercially available one-dimensional, dispersive hyperspectral imager [14] (DHI) so that the linear array of optical fibres at its output constitutes the input slit of the device. Ofner relay reflective optics and a holographic diffraction grating within the DHI form a spectrally dispersed image of the linear array on a low-noise cooled CCD. Computer algorithms invert the pixel mapping of the fibre optic reformatter to produce a hyperspectral data cube of the foveal region of the image.

### 2.2. Design and practical implementation of FHI

The FOR [15] was constructed from a coherent array of ribbon fibres, each ribbon consisting of seven constituent fibres. The reformatter mapped a  $14 \times 14$  array of fibres into a one-dimensional  $1 \times 196$  array. The optical fibres were  $50 \mu\text{m}$  in diameter and arranged on a  $56 \mu\text{m}$  pitch. The fibre numerical aperture of 0.1 was a good match to the  $f/2$  optics of the DHI. The combined effect of the area fill factor and Fresnel losses from the fibre ends limit the overall transmission of the FOR to 45%. Measured transmission of the FOR for white-light,  $f/2$  illumination demonstrated a fibre-to-fibre variation of 13% in transmission.

The DHI employs unity magnification, Ofner relay optics and a holographic diffraction grating that yields less than 0.1% smile and keystone distortion of recorded spectra. We measured 21% transmission efficiency into the first-order dispersed image. The spectral resolution of the FHI system is limited by the convolution of the point-spread function of the imager with the footprints of the input fibres and of the CCD pixels. In the demonstration system, the diameter of the fibres at the input to the DHI is the dominant factor, limiting the spectral resolution to 5 nm. The dispersed image at the CCD is sampled with a pixel pitch of  $6 \mu\text{m}$  giving a spectral bin every 0.6 nm. The assembled CCD, DHI and FOR are shown in figure 2.

The combination of FOR, DHI and CCD provides a fovea with  $14 \times 14$  pixels spatially, and 500 spectral bins within the range 400–700 nm. In general, diffractive spectrometers require the use of spectral filtering to restrict the spectral range to less than one octave to prevent overlapping of diffraction

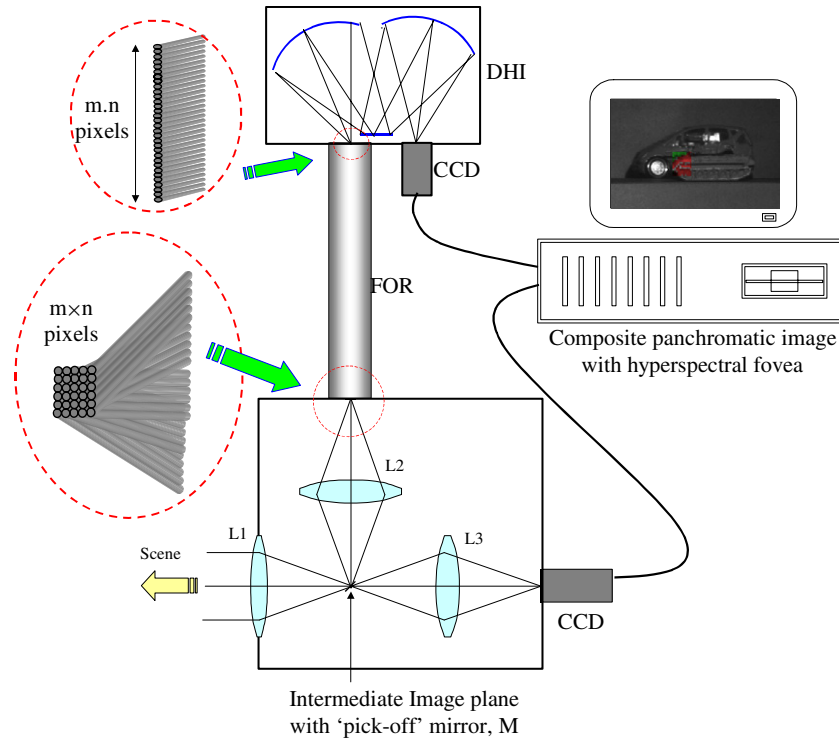


**Figure 1.** A schematic diagram of the instrument described. One camera is used to record a wide-field, panchromatic peripheral image, while another records a reformatted, spectrally dispersed image, which is used to form a hyperspectral fovea.

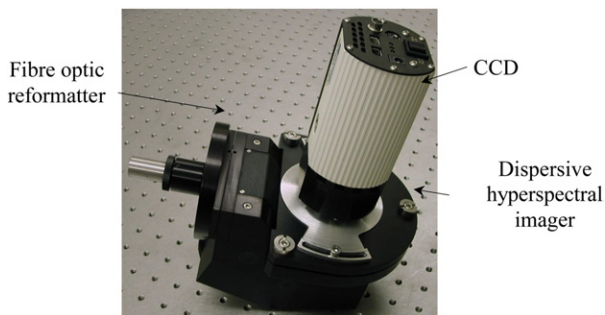


**Figure 2.** A photograph of the assembly of image reformatter, dispersive one-dimensional imaging spectrograph and cooled CCD camera.

orders. For our proof-of-principle experiments this was accomplished by filtering of the light source.

The optical fibre reformatter is clearly a limitation, in terms both of the relatively modest total number of foveal pixels and of the reduced spectral resolution due to the relatively thick fibres. Furthermore, for the unity magnification of the Ofner relay, the diameter of the fibres limits the maximum number of pixels that can be imaged onto commonly available large-format CCDs. Reduction of the fibre diameter to, for example,  $10\ \mu\text{m}$  would enable a fovea with a significantly improved spatial resolution of  $70 \times 70$  pixels and a spectral resolution of  $1\ \text{nm}$ . Due to the fragility of such thin fibres, construction of such a formatter will be difficult and expensive. In principle, there will be optical cross-coupling of light between neighbouring fibres that will introduce some blurring. This effect could be corrected by appropriate inversion techniques, but we found the cross-coupling not to be of significant magnitude to warrant this additional complexity.

### 2.3. FHI calibration and demonstration

The FHI demonstration system employed a simple co-aligned, side-by-side arrangement of cameras in place of the pick-off mirror arrangement shown in figure 1. Both cameras were controlled by a PC running Labview [16], which was also used for calibration and assembly of foveal images. A typical dispersed image, as recorded by the detector, is shown in figure 3; this shows the spectrally dispersed image of the linear array of 192 fibre ends at the input to the DHI.

Calibration of the FOR and DHI, when combined as a system, is required to correct for irregularities in the positioning of the optical fibres and to correct for relative fibre-to-fibre variations in the optical transmission. The root mean square deviation of the fibre images from their nominal positions was determined to be  $20\ \mu\text{m}$ . The mean spectral dispersion for all fibres was calibrated using illumination by HeNe laser light at  $632.8$  and  $543.5\ \text{nm}$  and spatial offsets due to irregularities in the one-dimensional fibre array were incorporated into the wavelength calibration for each fibre. The CCD pixels corresponding to the width of each fibre were summed into a single spectral bin. The spectral throughput of the assembled system was calibrated by imaging defocused calibrated reflectance tiles [17] under uniform illumination onto the FOR input face.

## 3. Spectral classification with the FHI

Processing of the foveal spectra consists of the comparison of the spectrum associated with each pixel with target spectra and the false colouring of classified pixels in the displayed image. Each pixel was classified as belonging to object A,

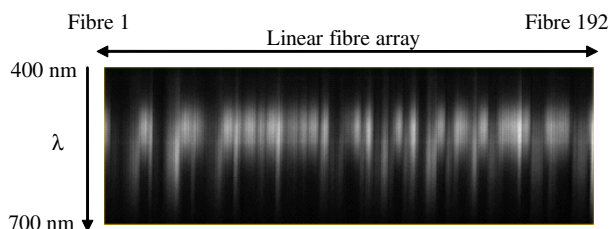


**Figure 3.** A typical spectrally dispersed image recorded on the foveal CCD.

object B or neither (therefore belonging to the background) based on a least-squares difference between the pixel spectrum and training spectra. To reduce the effects of variations in illumination intensity and direction, the magnitudes of all spectra were normalized for minimum RMS difference with the training spectra. A false-colour image was generated in which pixels were attributed a red or blue hue if they were classified as having spectra similar to training spectra for objects A and B respectively. Pixels with spectra dissimilar to the target spectra retained a neutral hue. The resulting false-colour foveal image was then embedded into the panchromatic peripheral image to produce a co-registered composite image.

Conventional images of an example scene including a model car and a model tank against a green background are shown in figure 4(a). The background spectrum was adjusted to be a close match to that of the tank. Measured spectra of the background, car and tank appear in figure 4(b). It can be seen that tank and background spectra are very similar, but dissimilar to the spectrum of the car. In figure 5 we show a single frame from a processed movie sequence recorded as the FHI is panned across the scene shown in figure 4. Image pixels classified as belonging to the same spectral classes as the car and tank were attributed red and green hues respectively; however, for compatibility with monochrome printing these hues have been replaced by white and hatched shading respectively. In the associated animation file (available at [stacks.iop.org/JOptA/7/S298](http://stacks.iop.org/JOptA/7/S298)) it is interesting to note that although there are relatively few pixels within the fovea, human perception appears to integrate the time sequence of hyperspectral foveal images into a more extended mental representation, indicating that even a small hyperspectral fovea may offer a very significant benefit.

#### 4. Conclusions

We have described a hyperspectral foveal imaging system that offers a solution to the fundamental problems of snapshot hyperspectral imaging in two dimensions and of the information bottleneck of detector arrays. The images presented in this paper together with the downloadable animation files illustrate the real-time recording and processing of hyperspectral image sequences to highlight specific target spectra within the scene. In our demonstration system, the frame-rate was approximately 4 Hz, but extension to video-rate foveal hyperspectral imaging will be unproblematic. It is envisaged that a typical mode of operation will involve the detection of regions of interest in the panchromatic periphery followed by scanning of the fovea to these regions for spectral classification. An additional and useful sophistication could

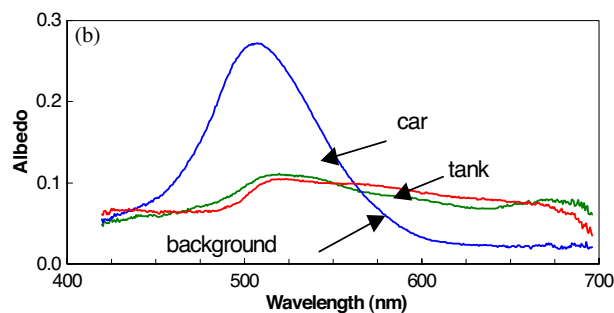


**Figure 4.** (a) A conventional, three-colour photograph of a scene consisting of a green model tank and a green model car against a background colour to be a close match to the colour of the tank and (b) the measured albedos of the three spectral classes.

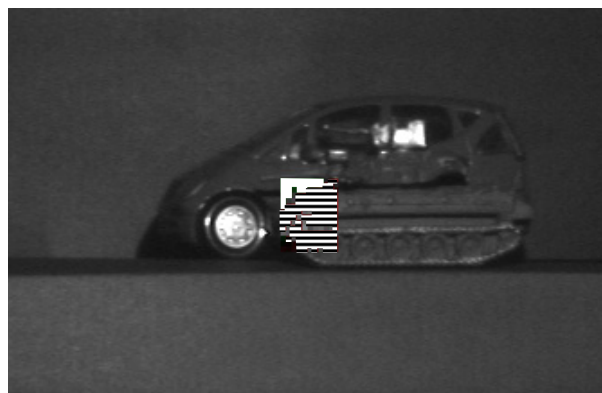


**Figure 5.** The image of the tank and car in the combined field of view. Pixels inside the fovea are assigned pure white or hatched to indicate similarity to training spectra for the car and tank respectively. Unclassified pixels retain greyscale values. This frame was taken from an animation that is available at [stacks.iop.org/JOptA/7/S298](http://stacks.iop.org/JOptA/7/S298).

involve the introduction of a memory so that the hyperspectral foveal classification is ‘painted’ over the panchromatic image during scanning to enable a wide-field image integration capability more similar to that demonstrated by the human visual system.

Since there is no time-sequential multiplex loss, the optical throughput (and hence also signal-to-noise ratio) is higher than for conventional techniques of equal resolving power. The optical efficiency is in practice dominated by the optical transmission of the FOR and of the DHI. This latter parameter could be improved by use of a prism in place of the holographic diffraction grating. Very importantly, the snapshot capability means that time-resolved hyperspectral imaging is possible and for imaging of moving scenes the commonly encountered spectral distortion is absent. An attractive future development

would be to use a FOR with smaller fibres since this will enable both higher spatial and higher spectral resolution. Applications where the real-time capability of foveal hyperspectral imaging shows particular promise include surveillance, retinal imaging and medicine.

## Acknowledgment

This work was carried out with funding from the Sensors and Electronic Warfare Research Domain of the UK MoD Corporate Research Programme.

## References

- [1] Boregaser M 2004 *Hyperspectral Remote Sensing* (Boca Raton, FL: Lewis)
- [2] Farkus D L 2001 *Methods in Cellular Imaging* ed A Periasamy, American Physiological Society (Oxford: Oxford University Press) chapter 20 (Spectral Microscopy for Quantitative Cell and Tissue Imaging) pp 345–61
- [3] Harvey A R and Fletcher-Holmes D W 2004 Birefringent two-dimensional Fourier-transform imaging spectrometer *Opt. Express* **12** 5368–74
- [4] Katz S, Dubinsky Z, Rothmann C, Malik Z and Friedlander M 1997 Single-cell pigmentation of *Porphyra linearis* analyzed by Fourier transform multi-pixel spectroscopy and image analysis *J. Phycol.* **33** 425–32
- [5] Lawlor J, Fletcher-Holmes D W, Harvey A R and McNaught A I 2002 *In vivo* hyperspectral imaging of human retina and optic disc *Invest. Ophthalmol. Vis. Sci.* **43** 4350
- [6] Hammer M, Thamm E and Schweitzer D 2002 A simple algorithm for *in vivo* ocular fundus oximetry compensating for non-haemoglobin absorption and scattering *Phys. Med. Biol.* **47** N233–8
- [7] Hunicz J and Piernikarski D 2001 Investigation of combustion in a gasoline engine using spectrophotometric methods *Optoelectronic and Electronic Sensors IV Proc. SPIE* vol 4516, ed J Fraczek (Bellingham, WA: SPIE Optical Engineering Press) pp 307–14
- [8] Kindzelskii A L, Yang Z Y, Nabel G J, Todd R F and Petty H R 2000 Ebola virus secretory glycoprotein (sGP) diminishes Fc gamma RIIIB-to-CR3 proximity on neutrophils *J. Immunol.* **164** 953–8
- [9] Harvey A R, Beale J, Greenaway A H, Hanlon T J and Williams J 2000 Technology options for imaging spectrometry *Imaging Spectrometry VI Proc. SPIE* vol 4132, ed M Descour and S Shen (Bellingham, WA: SPIE Optical Engineering Press) pp 13–24
- [10] Descour M R and Dereniak E R 1995 Computed tomography imaging spectrometer: experimental calibration and reconstruction results *Appl. Opt.* **34** 4817–26
- [11] Harvey A R and Fletcher-Holmes D W 2005 Generalization of the Lyot filter for snapshot spectral imaging in 2 dimensions *Opt. Lett.* submitted
- [12] Harvey A R and Fletcher-Holmes D W 2003 Imaging spectrometer *Patent Specification* WO03/089890 A1
- [13] Ren D Q and Allington-Smith J 2002 On the application of integral field unit design theory for imaging spectroscopy *Publ. Astron. Soc. Pac.* **114** 866–78
- [14] HyperSpec VS-15 manufactured by American Holographic Inc. (now Headwall Photonics Inc.), 601 River Street, Fitchburg, MA 01420, USA (<http://63.101.74.184/>)
- [15] Fibreoptic Systems Inc., 60 Moreland Rd, Unit A, Simi Valley, CA 93065, USA (<http://www.fibopsys.com/>)
- [16] National Instruments Corporation, 11500 N Mopac Expwy, Austin, TX 78759-3504, USA (<http://www.labview.com/>)
- [17] Labsphere Inc., North Sutton, NH 03260, USA (<http://www.labsphere.com/>)